International Journal of Heat and Mass Transfer 53 (2010) 3593–3606

Contents lists available at ScienceDirect

International Journal of Heat and Mass Transfer

journal homepage: www.elsevier.com/locate/ijhmt

Time periodic flow boiling heat transfer of R-134a and associated bubble characteristics in a narrow annular duct due to flow rate oscillation

C.A. Chen, W.R. Chang, T.F. Lin *

Department of Mechanical Engineering, National Chiao Tung University, Hsinchu, 1001 Ta Hsueh Road, Hsinchu 30010, Taiwan, ROC

ARTICLE INFO

Article history:
Received 30 June 2009
Received in revised form 22 January 2010
Accepted 22 January 2010
Available online 13 June 2010

Keywords:
Time periodic flow boiling
R-134a boiling heat transfer
Intermittent boiling
Flow rate oscillation

ABSTRACT

An experiment is conducted here to investigate the effects of the imposed time periodic refrigerant flow rate oscillation in the form of nearly a triangular wave on refrigeriant R-134a flow boiling heat transfer and associated bubble characteristics in a horizontal narrow annular duct with the duct gap fixed at 2.0 mm. The results indicate that when the imposed heat flux is close to that for the onset of stable flow boiling, intermittent flow boiling appears in which nucleate boiling on the heated surface does not exist in an entire periodic cycle. At somewhat higher heat flux persistent boiling prevails. Besides, the refrigerant flow rate oscillation only slightly affects the time-average boiling curves and heat transfer coefficients. Moreover, the heated wall temperature, bubble departure diameter and frequency, and active nucleation site density are found to oscillate periodically in time as well and at the same frequency as the imposed mass flux oscillation. Furthermore, in the persistent boiling the resulting heated wall temperature oscillation is stronger for a longer period and a larger amplitude of the mass flux oscillation. And for a larger amplitude of the mass flux oscillation, stronger temporal oscillations in the bubble characteristics are noted. The effects of the mass flux oscillation on the size of the departing bubble and active nucleation site density dominate over the bubble departure frequency, causing the heated wall temperature to decrease and heat transfer coefficient to increase at reducing mass flux in the flow boiling, opposing to that in the single-phase flow. But they are only mildly affected by the period of the mass flux oscillation. However, a short time lag in the wall temperature oscillation is also noted. Finally, a flow regime map is provided to delineate the boundaries separating different boiling regimes for the R-134a flow boiling in the annular duct.

1. Introduction

Improving energy utilization efficiency in engineering systems is receiving ever increasing attention worldwide intending to reduce the release of CO_2(g), a global weather warming gas. Recently, the use of variable frequency, instead of ON/OFF, compressors in various air conditioning and refrigeration systems to meet the temporally changing thermal load has been found to significantly augment their energy efficiencies. In these systems the refrigerant flow rate varies with time and the systems are subjected to changing thermal load. How the time dependent refrigerant flow rate and heat flux affect the characteristics of boiling and condensation processes in the refrigeration cycles employed in these systems remains largely unexplored. Besides, in cooling future ultra-high component density electronic devices, methods based on the phase change heat transfer are often considered. Moreover, the power dissipated in these devices is also time dependent and hence the cooling load. The associated time dependent two-phase flow and heat transfer processes are also poorly understood.

Flow boiling of refrigerants at constant flow rate in small ducts has received some attention. About a decade ago flow boiling of refrigerants R-11 and R-123 in a horizontal small tube (D_h = 1.95 mm) investigated by Bao et al. [1] showed that the heat transfer coefficients were independent of the refrigerant mass flux and vapor quality, but were a strong function of the wall heat flux. Nucleate boiling was noted to be the dominant mechanism. A similar study from Tran et al. [2] for R-12 reports two distinct two-phase flow regions – the convective boiling dominant region at lower ΔT_{sat} (<2.75 K) and nucleate boiling dominant region at higher ΔT_{sat} (>2.75 K). For R-134a in an upward vertical rectangular multi-channel Agostini and Bontemps [3] noted that bubble nucleation was the dominant mechanism for $q > 14$ kW/m^2 and $\Delta T_{sat} > 3$ K, and the transition from the boiling dominated by nucleation to convection occurred at $Bo(1-x) \approx 2.2 \times 10^{-4}$. Kandlikar and Steinke [4] found that for a high liquid-to-vapor density ratio, the convective effects dominated as the vapor quality increased. This led to an increasing trend in the boiling heat transfer at increasing x. A high boiling number results in a higher nucleate boiling contribution, which tends to

* Corresponding author. Tel.: +88 63515 71212x55101; fax: +88 63515 720634.
E-mail address: tfline@mail.nctu.edu.tw (T.F. Lin).

0017-9310/$ - see front matter © 2010 Published by Elsevier Ltd.
doi:10.1016/j.ijheatmasstransfer.2010.02.038

Nomenclature

A_s	outside surface area of the heated inner pipe (m^2)
A_{Tw}	amplitude of the heated wall temperature oscillation (°C)
Bo	Boiling number, $Bo = \frac{q}{G \cdot i_{fg}}$ (dimensionless)
$\overline{Bo}$	time-average Boiling number, $\overline{Bo} = \frac{q}{\overline{G} \cdot i_{fg}}$ (dimensionless)
D_i, D_o	inner and outside diameters of duct (m)
D_h	hydraulic diameter, $D_h = (D_o - D_i)$ (m)
d_P	bubble departure diameter (m)
f	bubble departure frequency
$G, \overline{G}$	instantaneous and time-average mass fluxes (kg/m^2 s)
h_r	boiling heat transfer coefficient (W/m^2 °C)
i_{fg}	enthalpy of vaporization (J/kg)
n_{ac}	active nucleation site density (n/m^2)
P, P_{in}	system pressure and inlet pressure (kpa)
q	imposed heat flux (W/m^2)
q_b	heat flux due to bubble nucleation (latent heat transfer) (W/m^2)
Q_n	net power input (W)
$\overline{Re}$	time-average Reynolds number of liquid flow, $\overline{Re} = \frac{\overline{G} D_h}{\mu_l}$ (dimensionless)
t_p	period of mass flux oscillation (s)
$T_{sat}, \overline{T}_{sat}$	instantaneous and time-average saturated temperature of refrigerant (°C)
T_w	temperature of heated wall for inner pipe (°C)
x	vapor quality
z	downstream coordinate measured from inlet of heated test section (mm)

Greek symbols

ΔG	amplitude of mass flux oscillation (kg/m^2 s)
ΔT_{sat}	wall superheat, $(T_w - T_{sat})$ (°C)
$\Delta \overline{T}_{sat}$	time-average wall superheat, $(\overline{T}_w - \overline{T}_{sat})$ (°C)
δ	gap size (mm)

decrease as x increases, causing a decreasing trend in h_r with increasing x. An experimental study for the flow boiling of refrigerant R-141b in a vertical tube conducted by Lin et al. [5] indicated that at low vapor quality nucleate boiling dominated. But at higher vapor quality convective boiling dominates. In a review article Watel [6] concluded that convective boiling dominated at low heat fluxes and wall superheats and high vapor qualities, otherwise nucleate boiling dominated.

For several decades, two-phase dynamic instabilities in the flow boiling of various liquids in a long heated channel have been recognized [7,8]. Significant temporal oscillations in pressure, temperature, mass flux and boiling onset occur at a certain operating condition. Specifically in flow boiling of R-11 in a vertical channel, the pressure-drop and thermal oscillations were observed by Kakac et al. [9]. The presence of the density wave oscillation superimposed on the pressure-drop oscillation was further noted by Kakac and his colleagues [10]. In a continuing study for R-11 in a horizontal tube of 106 cm long, they [11] examined the dependence of the oscillation amplitude and period on the system parameters and located the boundaries for various types of oscillations. A similar experimental study was carried out by Comakli et al. [12] and the effect of the channel length on the two-phase flow dynamic instabilities was examined.

The dynamic behavior for a horizontal boiling channel connected with a surge tank for liquid supply has received some attention [13]. The boiling onset in an upward flow of subcooled water in a vertical tube of 7.8-m long connected with a liquid surge tank could cause substantial flow pressure and density-wave oscillations [14]. These boiling onset oscillations were attributed to a sudden increase of pressure-drop across the channel and a large fluctuation in the water flow rate at the onset of nucleate boiling. This in turn results from the feedback of the pressure-drop and flow rate by the system, causing the location of the boiling onset to move in and out of the channel. The pressure-drop oscillation of n-pentane liquid in a vertical small rectangular channel ($D_h = 0.889$ mm) was reported by Brutin et al. [15]. The effects of the inlet flow conditions on the boiling instabilities were found to be relatively significant [16]. A similar study for subcooled flow boiling of deionized water was conducted by Shuai et al. [17] and the pressure-drop oscillation was also noted. Reviews of two-phase flow dynamic instabilities in tube boiling have been conducted recently by Kakac and Bon [18] and Tadrist [19].

It has been known for some time that bubble characteristics such as bubble departure frequency, growth, sliding and departure size play an important role in flow boiling heat transfer. Yin et al. [20] examined some bubble characteristics associated with stable subcooled flow boiling of R-134a in a horizontal annular duct. They noted that the bubble departure frequency was suppressed by raising the mass flux and subcooling of R-134a, and only the liquid subcooling significantly affected the bubble size. Visualization of stable subcooled flow boiling of upward water flow in a vertical annular channel by Situ et al. [21] suggested that generally the bubble departure frequency increased with the heat flux and the bubble growth rate dropped sharply after the bubble lift-off. The study of stable water boiling in a horizontal rectangular channel conducted by Maurus et al. [22] manifested that the waiting time between two bubble cycles decreased significantly at increasing mass flux. Chang et al. [23] studied the near-wall bubble behavior for water in a vertical one-side heated rectangular channel. They showed that the size of coalesced bubbles decreased for an increase in the water mass flux and the mass flux only exhibits a strong effect on the bubble size. Del Balle and Kenning [24] examined the stable subcooled flow boiling for water in a rectangular vertical channel and found that the maximum bubble diameter was independent of the heat flux. An experimental study on the bubble rise path after its departure from a nucleation site for water in a vertically upward tube by Okawa et al. [25] suggested that the inertia force significantly influenced the onset of bubble detachment and the shear force induced a lift force to detach the bubble from the wall.

The above literature review clearly indicates that the unsteady flow boiling heat transfer of HFC refrigerants in small diameter channels resulting from time varying mass flux and/or heat flux remains largely unexplored. In a recent study [26], we measured the stable saturated flow boiling heat transfer data and investigated the associated bubble characteristics for R-134a in a horizontal narrow annular duct. In the present study we move further to investigate the R-134a flow boiling in the same duct subject to a time periodic mass flux oscillation with a constant imposed heat flux. The effects of the imposed heat flux, amplitude and period of the mass flux oscillation, and refrigerant saturated temperature on the temporal boiling heat transfer characteristics will be examined in detail. Particularly, flow visualization is conducted to examine the bubble characteristics associated with the time periodic flow boiling, intending to

improve our understanding of the unsteady flow boiling processes in a narrow channel.

2. Experimental apparatus and procedures

The experimental system modified slightly from that used in the previous study [26] for stable flow boiling is also employed here to investigate the time periodic flow boiling of R-134a in a narrow annular duct. It is schematically depicted in Fig. 1. The experimental apparatus consists of three main loops, namely, a refrigerant loop, a water–glycol loop, and a hot-water loop. Refrigerant R-134a is circulated in the refrigerant loop. In order to control various test conditions of the refrigerant in the test section, we need to control the temperature and flow rate in the other two loops. The system is already described in detail there [26]. The temporal oscillation of the refrigerant flow rate is implemented by an external control of an inverter connecting to a refrigerant pump through a programmable DC current or voltage signal sequence.

As schematically shown in Fig. 2, the test section is a horizontal annular duct with the outer pipe made of Pyrex glass to permit the visualization of boiling processes in the refrigerant flow. The glass pipe is 160-mm long with an inside diameter of 20.0 mm. Its wall is 4.0-mm thick. Both ends of the pipe are connected with copper tubes of the same size by means of flanges and are sealed by O-rings. The inner copper pipe has 16.0 mm nominal outside diameter with its wall being 1.5 mm thick and is 0.41-m long. Thus the gap of the annular duct is 2.0 mm (D_h = 4.0 mm). Note that the outside surface of the inner pipe is polished successively by fine sandpapers of Nos. 1000, 2000, 3000 and then cleaned by ethanol. In order to insure the gap between the inner and outer pipes being uniform, we first measure the outside diameter of the inner pipe and the inside diameter of the glass pipe by digital calipers whose resolutions are 0.001 mm with the measurement accuracy of ±0.01 mm. Then we photo the top and side view pictures of the annular duct and measure the average radial distance between the inside surface of the glass pipe to the outside surface of the inner tube. From the above procedures the duct gap is ascertained and its uncertainty is estimated to be 0.02 mm. It is also noted that the flow enters the duct long before the heated section with the entry length of 93 mm so that the entrance effects on the boiling are small. An electric cartridge heater of 160 mm in length and 12.5 mm in diameter with a maximum power output of 800 W is inserted into the inner pipe. Furthermore, the pipe has an inactive heating zone of 10-mm long at each end and is insulated with Teflon blocks and thermally nonconducting epoxy to minimize heat loss from it. Thermal contact between the heater and the inner pipe is improved by coating a thin layer of heat-sink compound on the heater surface before the installation of the heater. Then, eight T-type calibrated thermocouples are electrically insulated by electrically nonconducting thermal bond before they are fixed on the inside surface of the inner pipe so that the voltage signals from the thermocouples are not interfered with the DC current passing through the cartridge heater. The thermocouples are positioned at three axial stations along the inner pipe. At each axial station, two to four thermocouples are placed at top, bottom, or two sides of the pipe circumference with 180° or 90° apart. The outside surface temperature of the inner pipe T_w is then derived from the measured inside surface temperature by taking into account the radial heat conduction through the pipe wall. In view of the relatively high thermal conductivity of copper, this approximate

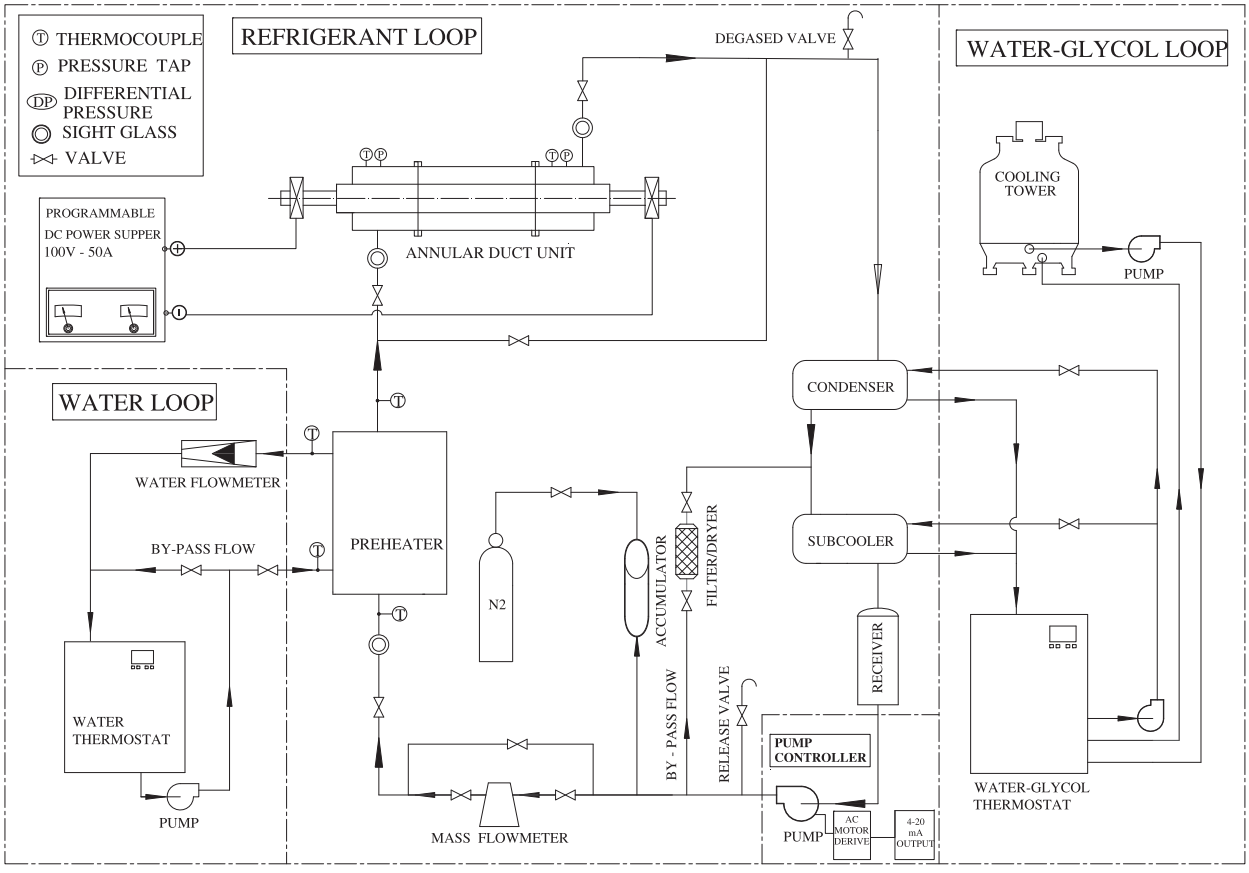

Fig. 1. Schematic of experimental system for flow boiling in annular duct.

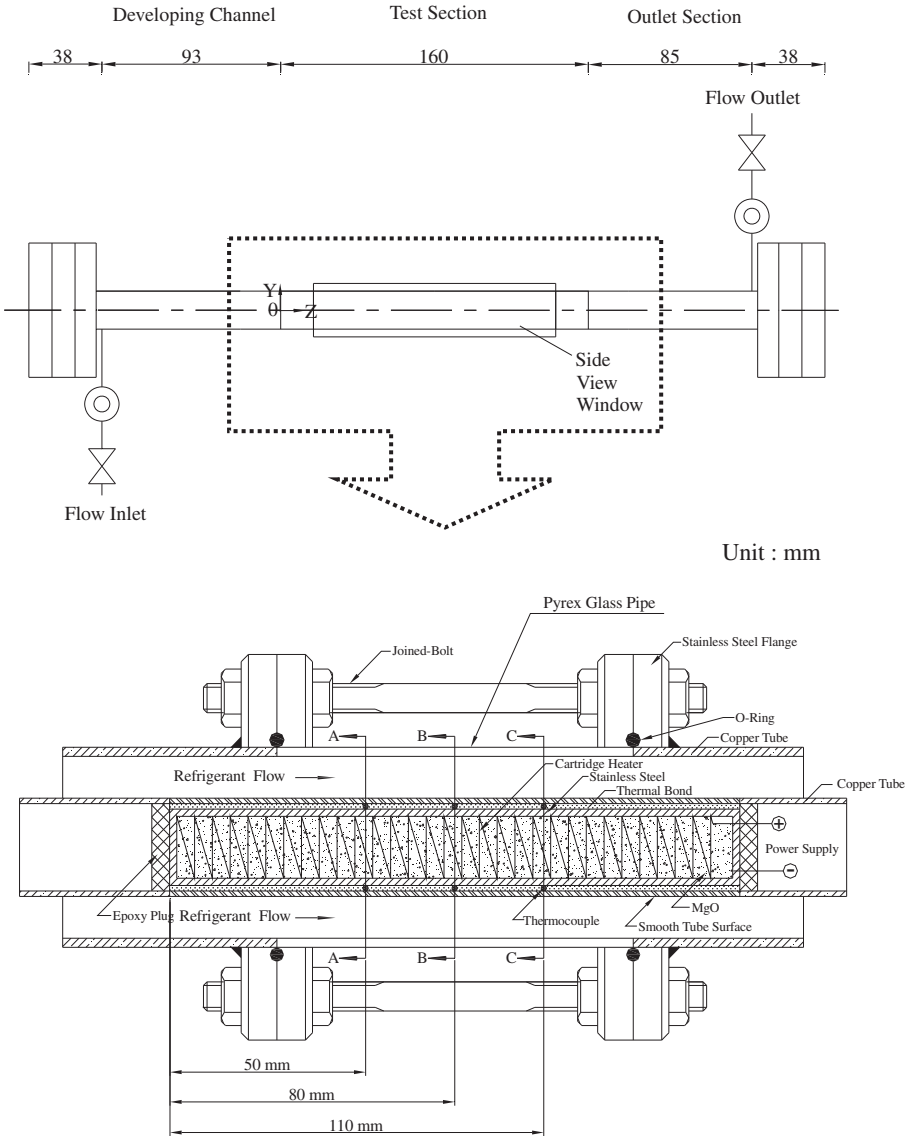

Fig. 2. The detailed arrangement of test section for annular duct.

evaluation of the heated wall temperature is found to result in an error smaller than 0.1 °C, when compared with the data derived from solving the transient heat conduction equation for the inner pipe wall by numerical computation.

The photographic apparatus established in the present study to record the bubble characteristics in the time periodic flow boiling in the annular duct consists of an IDT X-Stream^{TM} VISION XS-4 high speed CMOS digital camera, a Mitutoyo micro lens set, a 3D positioning mechanism, and a personal computer. The high-speed digital camera can take photographs up to 143,307 frames/s with an image resolution of 512×16. Here, a recording rate of 10,000 frames/s with the highest image resolution of 512×256 is adopted to obtain the images of the bubble ebullition processes in the flow boiling. The data for some bubble characteristics are collected in a small region around the middle axial location ($z = 80$ mm). After the experimental system reaches a statistical state, we start recording the boiling activity. The high-speed digital camera can store the images which are later downloaded to the personal computer. Then, the time variations of the space-average bubble departure diameter and frequency and active nucleation site density in a periodic cycle are calculated by viewing more than 1000 frames at each time instant. More specifically, the bubble departure diameter and frequency are respectively evaluated by measuring the diameters and numbers of bubbles departing from a few nucleation sites over a time interval much longer than the bubble departure period and much shorter than the mass flux oscillation period. Besides, the active nucleation site density is estimated by counting number of bubble nucleation sites over a small heated surface area over the same small time interval.

Before a test is started, the temperature of refrigerant R-134a in the test section is compared with its saturation temperature corresponding to the measured time-average saturation pressure and the allowable difference is kept in the range of 0.2–0.3 K. Otherwise, the system is re-evacuated and then re-charged to remove the air existing in the refrigerant loop. A vacuum pump is used to evacuate noncondensable gases in the system to a low pressure of 0.067 pa in the loop. In the test the refrigerant at the inlet of the test section is first maintained at the liquid state ($x = 0$) and its temperature is kept at the time-average saturated temperature corresponding to the time-average refrigerant pressure by adjusting the water–glycol temperature and flow rate. In addition, we adjust the thermostat temperature

in the water loop to stabilize the inlet refrigerant temperature. Then, we regulate the time-average refrigerant pressure at the test section inlet by adjusting the opening of the gate valve locating right after the exit of the test section. Meanwhile, by controlling the inverter current of the AC motor connecting to the refrigerant pump, the refrigerant flow rate can be varied to procure the preset mean level and the chosen period and amplitude of the mass flux oscillation. Specifically, due to the flow intertia the refrigerant flow rate varies like a triangular wave. The imposed heat flux from the heater to the refrigerant is adjusted by varying the electric current delivered from the programmable DC power supply. By measuring the current delivered to and voltage drop across the heater and by photographing the bubble activity, we can calculate the heat transfer rate to the refrigerant and obtain the bubble characteristics. All tests are run at statistical conditions. The whole system is considered to be at a statistical state when the variations of the time-average system pressure and imposed heat flux are respectively within ±1% and ±4%, and the variations of the time-average heated wall temperature are less than ±0.2 °C for a period of 100 min. Then all the data channels are scanned every 0.05 s for a period of 360 s.

3. Data reduction and verification of experimental system

The imposed heat flux q to the refrigerant flow in the narrow annular duct is calculated on the basis of the net power input Q_n and the total outside surface area of the inner pipe of the annular duct A_s as $q = Q_n/A_s$. The total power input Q_t is obtained from the product of the measured voltage drop across the cartridge heater and electric current passing through it. Hence the net power input to the test section is equal to $(Q_t - Q_{loss})$.

The total heat loss from the test section Q_{loss} is evaluated from the correlation for natural convection around a circular cylinder by Churchill and Chu [27]. To reduce the heat loss from the test section, it is covered with a polyethylene insulation layer. The results from the present heat loss test indicate that the total heat loss from the test section is generally less than 1% of Q_t no matter when single-phase flow or two-phase boiling flow is in the duct. The flow boiling heat transfer coefficient at a given axial location at a given time instant is defined as

$$h_r = \frac{Q_n/A_s}{(T_w - \overline{T}_{sat})} \tag{1}$$

Uncertainties of the imposed heat flux and measured heat transfer coefficients are estimated according to the procedures proposed by Kline and McClintock [28] for the propagation of errors in physical measurement. The results from this estimate show that the uncertainties of the dimension, temperature, pressure, mean mass flux, period of oscillation, amplitude of oscillation, imposed heat flux, and boiling heat transfer coefficient measurements are less than ±1%, ±0.2 °C, ±0.2 kPa, ±2%, ±0.25 s, ±4.8%, ±4.5%, and ±14.5%, respectively.

In order to check the suitability of the experimental system for measuring the flow boiling heat transfer coefficients, the steady state single-phase liquid R-134a heat transfer coefficients for a constant liquid Reynolds number ranging from 3648 to 11,420 are measured first and compared with the well-known traditional forced convection correlation proposed by Gnielinski [29], as that in the previous study [26]. The results manifest that the present steady heat transfer data can be well correlated by his correlation with a mean absolute error of 3.9%. Because of the lack of the unsteady turbulent forced convection heat transfer data in the open literature, direct validation of the present time periodic liquid heat transfer data is not possible.

4. Results and discussion

The present time periodic R-134a flow boiling experiment is performed for the mean refrigerant mass flux $\overline{G}$ varying from 300 to 500 kg/m^2 s, imposed heat flux q from 0 to 45 kW/m^2, and mean system pressure $\overline{P}$ set at 414.6 kPa and 488.6 kPa (corresponding to the mean R-134a saturation temperature $\overline{T}_{sat} = 10$ °C and 15 °C) for the gap of the duct δ = 2.0 mm. Besides, the amplitude of the refrigerant mass flux oscillation ΔG is set at 0%, 10%, 20%, and 30% of $\overline{G}$. Moreover, the period of the mass flux oscillation t_p is fixed at 20, 30, 60, and 120 s. The ranges of the parameters chosen above for the mass flux oscillation are in accordance with the practical operation of variable speed compressors in some air-conditioners and refrigerators subject to fast changing thermal load. In the following, attention will be mainly paid to examining the effects of the amplitude and period of the refrigerant mass flux oscillation on the time periodic R-134a flow boiling heat transfer performance. Note that for the limiting case of $\Delta G/\overline{G} = 0\%$ we have saturated flow boiling of R-134a at a constant refrigerant mass flow rate in the test section, which is designated as stable flow boiling and has been investigated by Lie and Lin [26]. The measured boiling heat transfer data are expressed in terms of the boiling curve and boiling heat transfer coefficient. The thermal characteristics of the time periodic flow boiling are illustrated by the time variations of the instantaneous heated pipe wall temperature and boiling heat transfer coefficient. Moreover, selected flow photos and data deduced from the images of the boiling processes are presented to show the bubble characteristics in the boiling flow.

The time constant t_c associated with the response of the heated wall temperature to the time dependent refrigerant flow rate is an important physical quantity in the time periodic flow boiling. It is measured directly here from the time response of T_w subject to a step change in the mass flux for various q. The measured data show that t_c is about 16.0 s which is known to mainly result from the thermal inertia of the heated pipe wall.

4.1. Time-average boiling curves and heat transfer coefficient

At first, the time-average boiling curves and heat transfer coefficients measured at the middle axial location (z = 80 mm) of the narrow annular duct for various amplitudes and periods of the refrigerant mass flux oscillation are examined. It is noted that the time-average boiling curves and heat transfer coefficients are not affected by the amplitude and period of the refrigerant mass flux oscillation to a significant degree. In fact, they are nearly the same as that for the stable boiling.

4.2. Time dependent flow boiling heat transfer characteristics

The time periodic flow boiling heat transfer characteristics for R-134a flow in the annular duct resulting from the periodic refrigerant mass flux oscillation are illustrated in Figs. 3 and 4 by presenting the time variations of the heated wall temperature and boiling heat transfer coefficients at the middle axial location in the statistical state for various $\overline{G}, \overline{T}_{sat}, \Delta G/\overline{G}, t_p$, and q. For clear illustration, the measured data for the variations of the refrigerant mass flux are also given here. The results manifest that when G oscillates periodically in time nearly like a triangular wave, significant temporal oscillations in T_w and h_r can occur. Note that the T_w and h_r oscillations are also periodic in time and are at the same frequency as the mass flux. Besides, the T_w and h_r oscillations get stronger for a higher amplitude and a longer period of the mass flux oscillation. However, the amplitude of the T_w oscillation varies nonmonotonically with the imposed heat flux. Note that single-phase forced convection prevails in the duct at a relatively low

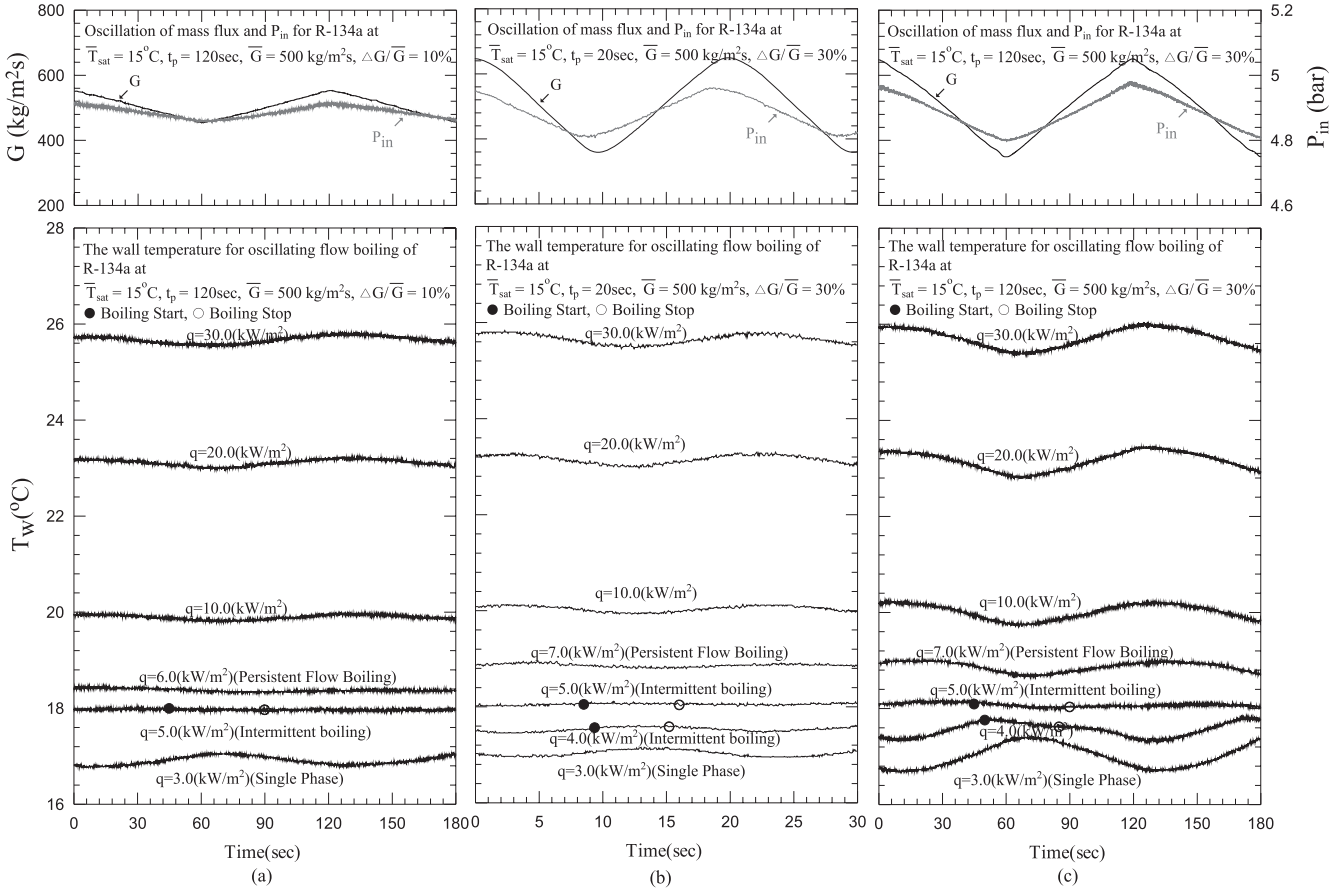

Fig. 3. Time variations of imposed mass flux, inlet pressure, and wall temperature at $z = 80$ mm for various q, $\Delta G/\overline{G}$ and t_p.

imposed heat flux. These data further reveal that the T_w and h_r oscillations slightly lag the mass flux oscillation, which apparently results from the thermal inertia of the heated pipe wall. Moreover for the single-phase convection at low q and in the first half of the periodic cycle in which the mass flux decreases with time, the wall temperature is found to rise with time, suggesting that the single-phase convection heat transfer over the heated surface is poorer at a lower G. The opposite process occurs in the second half of the cycle. It is further noted in the experiment that at a low q the wall temperature of the heating surface is lower than that required for the onset of nucleate boiling and no bubble nucleates from the heating surface. As the imposed wall heat flux is raised gradually, the wall temperature increases correspondingly. The corresponding T_w oscillation can be significant, as evident from the curve for $q = 3.0$ kW/m^2 in Fig. 3(c). At a certain higher wall temperature for a small increase in q bubbles start to nucleate from the heated surface at certain instant of time but bubble nucleation is not seen in the whole cycle. Thus, we have intermittent boiling in the flow in which nucleate boiling only exists in partial duration of the periodic cycle. The time instants for the start and termination of the nucleate boiling are marked on the curves for T_w for the cases with the intermittent boiling. At this intermediate imposed heat flux the T_w oscillation is very weak. In fact, for most cases the amplitude of T_w oscillation is smaller than 0.2 °C. For some increase in the imposed heat flux nucleate boiling persists over the entire period of the cycle and we have persistent flow boiling in the duct. It is of interest to note that at this higher q in the first half of the cycle in which G decreases with time, T_w also decreases with time, suggesting that the flow boiling heat transfer over the heated surface is better at a lower G, as supported by the data for h_r (Fig. 4). This trend is opposite to that for the single-phase convection. The results in Fig. 4 also show that the amplitude of h_r oscillation is not affected by the imposed heat flux in the persistent boiling to a noticeable degree. The appearance of the intermittent nucleate boiling and the improvement of boiling heat transfer by reducing G in the persistent boiling are somewhat unusual.

In this transient oscillatory boiling flow the time variations of the refrigerant pressure at the inlet of the test section are also shown in Figs. 3 and 4 for selected cases. The results indicate that P_{in} oscillates nearly in phase with G and also in the form of triangular waves. A close inspection, however, reveals that the mass flux oscillates slightly behind the pressure. Besides, the corresponding oscillation in the refrigerant saturated temperature is found to vary from 0.2 °C to 1.1 °C for all cases tested here. Specifically, in the first half of the periodic cycle in which G decreases with time the R-134a saturated temperature also decreases with time. Thus the R-134a liquid at the test section inlet which is kept at a constant level is at a superheated state and we have flow boiling in a superheated liquid. The resulting boiling heat transfer is hence improved. While in the second half of the cycle the opposite processes take place and we have boiling in a subcooled liquid. The resulting boiling heat transfer is hence poorer.

Finally, we move further to present the data in Fig. 5 to elucidate the effects of the experimental parameters on the amplitude of the T_w oscillation over a wide range of the imposed heat flux. The results for the high mean mass flux of 500 kg/m^2 s shown in Fig. 5(a) indicate that in the single-phase flow the oscillation amplitude of T_w increases significantly with the imposed heat flux for a given $\Delta G/\overline{G}$. Note that when the intermittent boiling appears

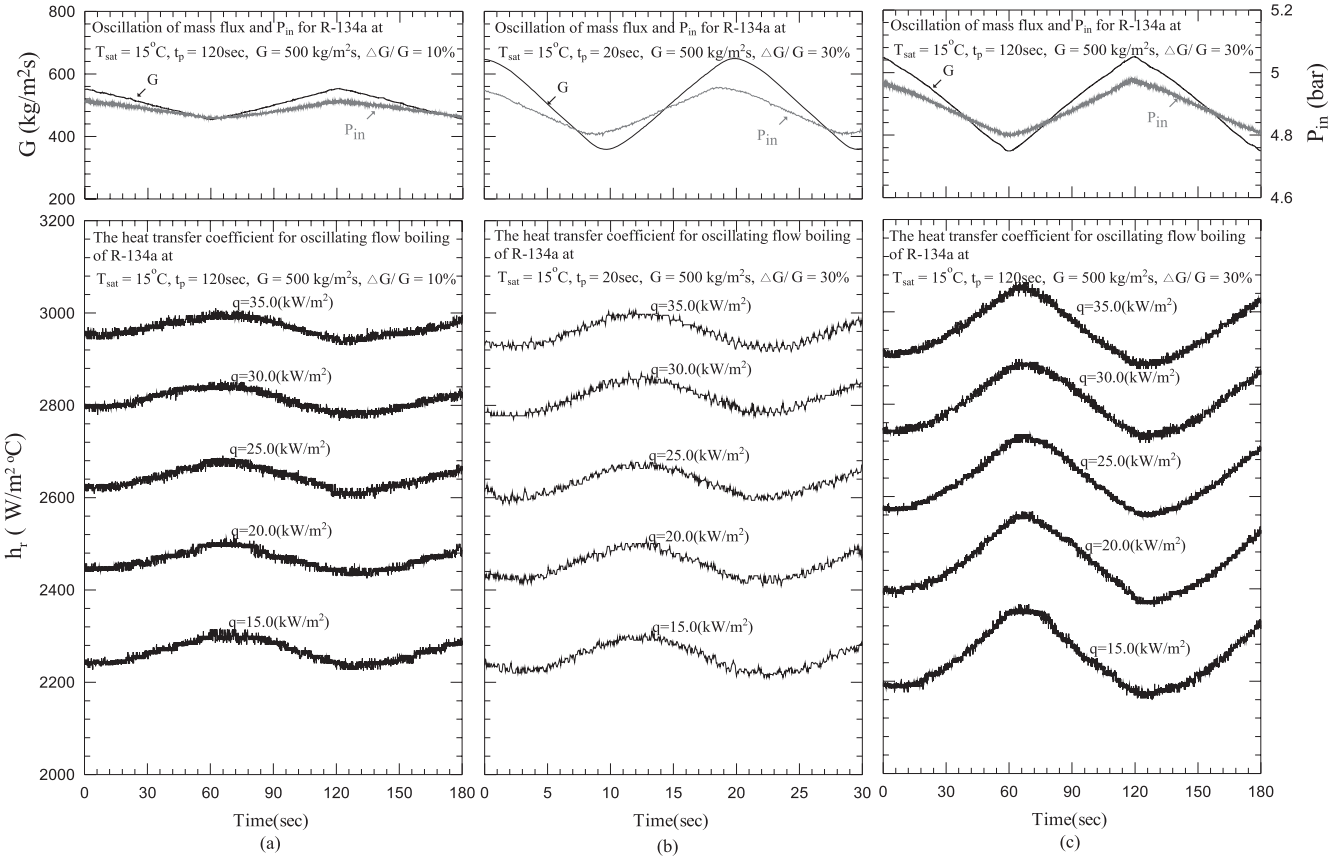

Fig. 4. Time variations of imposed mass flux, inlet pressure, and heat transfer coefficient at $z = 80$ mm in persistent boiling for various q, $\Delta G/\overline{G}$ and t_p.

the T_w oscillation starts to weaken substantially with the increase in the imposed heat flux. At a certain higher q but still in the intermittent boiling regime the T_w oscillation decays to a minimum point and then a further increase in q causes T_w to oscillate in a larger amplitude. This nonmonotonic variation of the T_w oscillation amplitude with q in the intermittent boiling can be attributed to the completely opposite trends in the T_w oscillation for the single-phase and boiling flows. Specifically, T_w increases as G decreases in the single-phase flow but in the boiling flow T_w decreases as G decreases. Thus as the bubble nucleation starts to appear in the single-phase flow the T_w oscillation is weakened. This trend continues until the effect of the boiling flow dominates over the single-phase flow for a rise in q to a certain level. Then, the T_w oscillation gets stronger for a higher q. In the persistent boiling regime at high imposed heat flux the T_w oscillation gets gradually stronger for a higher q up to about $q = 30$ kW/m^2. Beyond that the T_w oscillation nearly levels off. It is worth to note from the data given in Fig. 5(a) that at the low $\overline{G}$ of 300 kg/m^2 s the increase of the T_w oscillation amplitude with q in the intermittent boiling is very substantial and the T_w oscillation decays noticeably at increasing q in the persistent boiling. This stronger T_w oscillation at a lower $\overline{G}$ is attributed to the associated stronger boiling ebullition on the heated surface with the accompanying weaker single-phase convection. While at the intermediate $\overline{G}$ of 400 kg/m^2 s the variation of the T_w oscillation amplitude with q is small in the persistent boiling regime. Specifically, at intermediate imposed heat flux in the intermittent and persistent boiling T_w oscillates in a larger amplitude at a lower $\overline{G}$ but the opposite trend prevails at high q in the persistent boiling. The results in Fig. 5 also indicate that the T_w oscillation is stronger for a higher amplitude and a longer period of the mass flux oscillation. At the low t_p of 20 s, which is only slightly larger than the time constant of the present system, the T_w oscillation is rather weak (Fig. 5(d)), reflecting that the heated wall is unable to respond instantly to the fast mass flux oscillation for a t_p around or below t_c. However, the mean saturated temperature of the refrigerant shows a relatively insignificant effect on the amplitude of the T_w oscillation (Fig. 5(b)). It is also noted that for all cases tested in the persistent boiling for $q > 10.0$ kW/m^2 the amplitude of the T_w oscillation is less that 10% of the wall superheat. But in the intermittent boiling A_{T_W} can be as high as 25% of ΔT_{sat}.

4.3. Intermittent flow boiling

It is of interest to note in the visualization of the boiling flow in the annular duct that over a certain intermediate range of the imposed heat flux the intermittent boiling appears. More specifically, in a typical periodic cycle bubble nucleation on the heated inner pipe is first seen at a certain time instant in the first half of the cycle as the imposed refrigerant mass flux decreases to a certain low level and the pipe wall temperature rises to exceed the wall superheat required for the onset of nucleate boiling. The boiling process continues for some time interval. At a certain later time instant in the second half of the cycle in which G increases and T_w decreases to the level below that required for the onset of nucleate boiling, bubble nucleation disappears and the boiling stops. Single-phase flow then prevails in the duct. The above processes of the intermittent flow boiling are repeatedly seen on the heated surface. The data in Fig. 5 clearly manifest that the appearance of the intermittent boiling substantially affects the intensity of the T_w oscillation. To be more clear, we mark the time instants at which boiling starts and stops in Fig. 3 on the curves for the cases with the presence of the intermittent boiling. The present data show that at a higher imposed

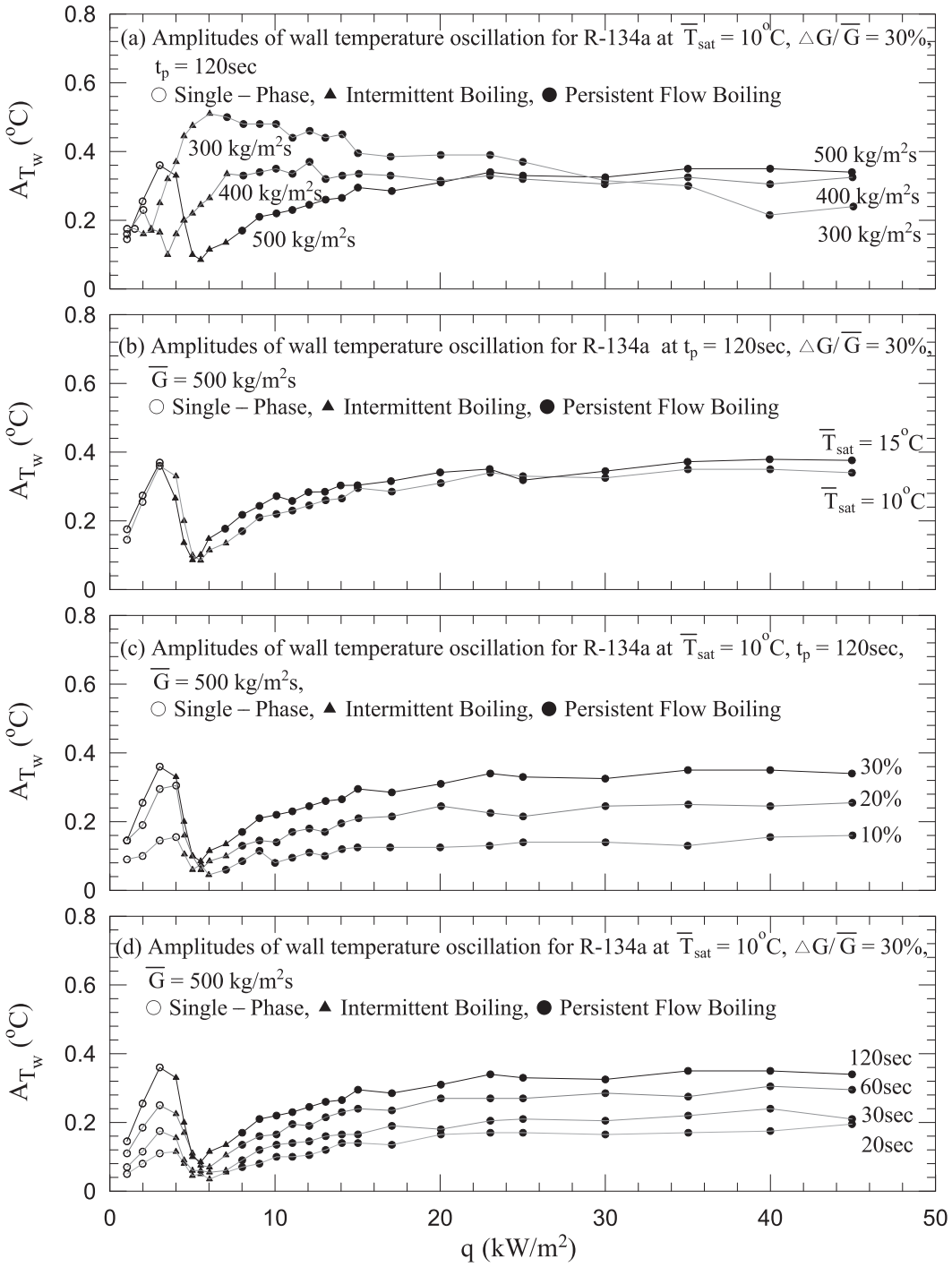

Fig. 5. Variations of amplitudes of heated wall temperature with imposed heat flux for various refrigerant mass fluxes (a), saturated temperatures (b), amplitudes of mass flux oscillation (c), and periods of mass flux oscillation (d).

heat flux and at a lower mean mass flux the onset of boiling is earlier and the termination of boiling is later. Besides, the instants for the boiling inception and termination are not affected by the period of the mass flux oscillation to a noticeable degree (Fig. 3). A flow regime map to delineate the boundaries separating different boiling regimes in terms of the Boiling number versus the relative amplitude of the mass flux oscillation is given in Fig. 6. The results show that the intermittent boiling prevails over a significantly wider range of the Boiling number for a higher amplitude of the mass flux oscillation and a lower mean saturated temperature of the refrigerant and for the mean refrigerant mass flux lowered from 500 to 400 kg/m² s by comparing the curves for different $\overline{T}_{sat}$ and $\overline{G}$. But for $\overline{G}$ reduced further from 400 to 300 kg/m² s the intermittent boiling dominates in a smaller range of the Boiling number except for $\Delta G/\overline{G}$ exceeding about 25%. Based on the present data, the conditions leading to the appearance of the intermittent boiling can be empirically correlated as

$$(-4.65\times10^{-5}+1.55\times10^{-6}\overline{Re}^{0.5}) \leqslant \frac{\overline{Bo}^{1.2}}{(\Delta G/\overline{G})^{2.5}} \leqslant (2.99\times10^{-3}+5.23\times10^{-6}\overline{Re}^{0.5}) \quad (2)$$

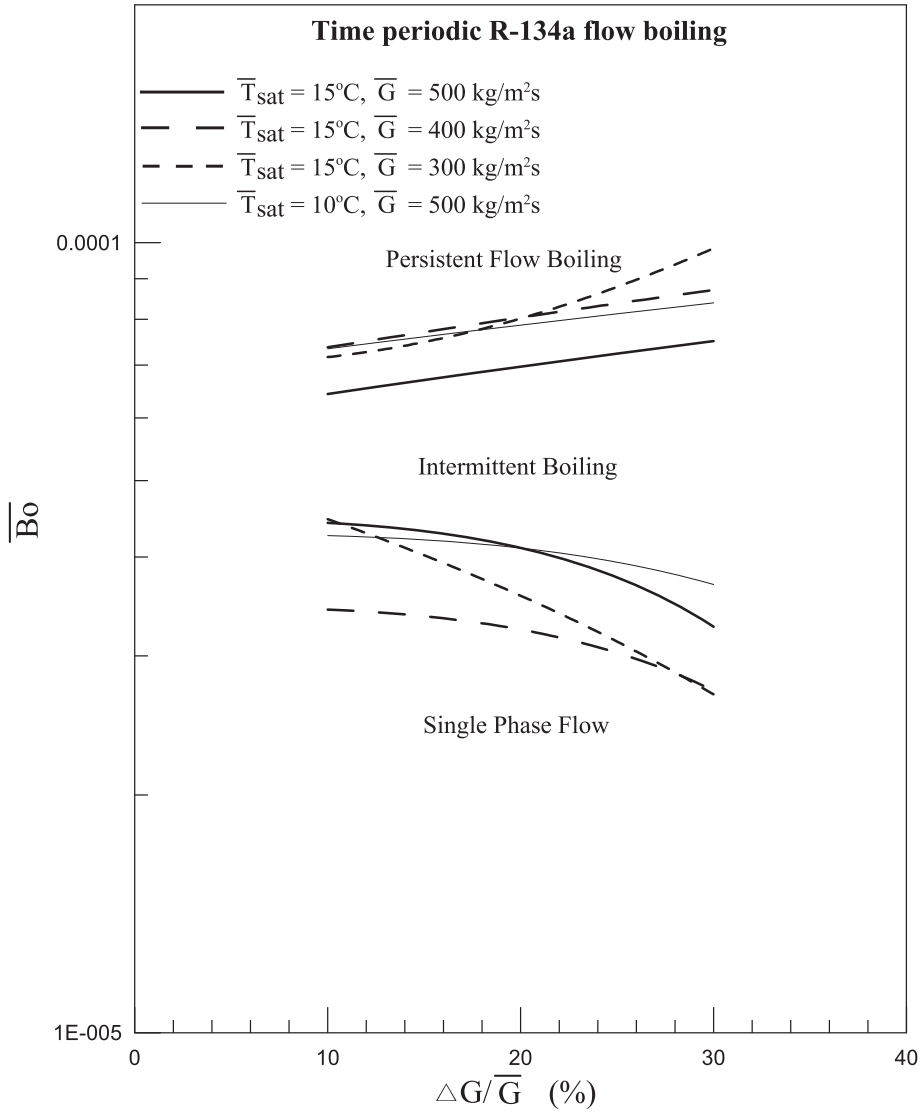

Fig. 6. Flow regime map for time periodic R-134a flow boiling in annular duct.

More than 96 % of the present data falls within the above correlation.

4.4. Bubble characteristics in time periodic flow boiling

The bubble characteristics associated with the stable saturated flow boiling of R-134a in the present narrow annular duct have been examined in our recent study [26]. These characteristics indicate that for the imposed heat flux exceeding that for onset of nucleate boiling the duct is dominated by the persistent boiling and a number of discrete bubbles nucleate from the cavities and slide along the heating surface. At a higher q the active bubble nucleation density increases and a lot of coalescence bubbles appear. More coalescence bubbles are seen and they are confined by the duct walls to become slightly deformed for a further increase in q. At even higher q the duct is mainly filled with the coalescence bubbles. They also reported that at a higher refrigerant mass flux the bubble departure frequency is higher and the bubbles are smaller and in violent agitating motion. However, the active nucleation site density is lower at a higher mass flux. But at the lower mass flux the bubble coalescence is more important and a number of bigger bubbles form in the duct. Then, at a lower saturation temperature of the refrigerant the bubbles were found to grow bigger and depart at a lower rate, and the active nucleation site density is lower due to the higher surface tension and enthalpy of vaporization.

By and large, in the time periodic flow boiling investigated here the effects of the imposed heat flux and mean refrigerant mass flux and saturation temperature on the bubble behavior are similar to that in the stable flow boiling. Hence, we illustrate here how the time periodic bubble characteristics are affected by the amplitude of the mass flux oscillation for the persistent boiling in Fig. 7 by presenting the photos of the boiling flow for the selected cases in a small region around the middle axial location at eight chosen time instants in a typical periodic cycle. In the figure the symbol "$t = t_o$" signifies the time instant at which the instantaneous refrigerant mass flux is at the highest level and starts to decrease. The results indicate that for given q, $\overline{G}$, $\Delta G/\overline{G}$, and t_p the bubbles get bigger and become more crowded in the duct in the first half of the cycle in which G decreases. The opposite processes take place in the second half of the cycle. These changes of the bubble characteristics with the instantaneous mass flux become more significant for an increase in the amplitude of the mass flux oscillation. Besides, we also note from the other photos not shown here that the bubble coalescence occurs more frequently and more large bubbles appear in the duct for the cases with a longer period of

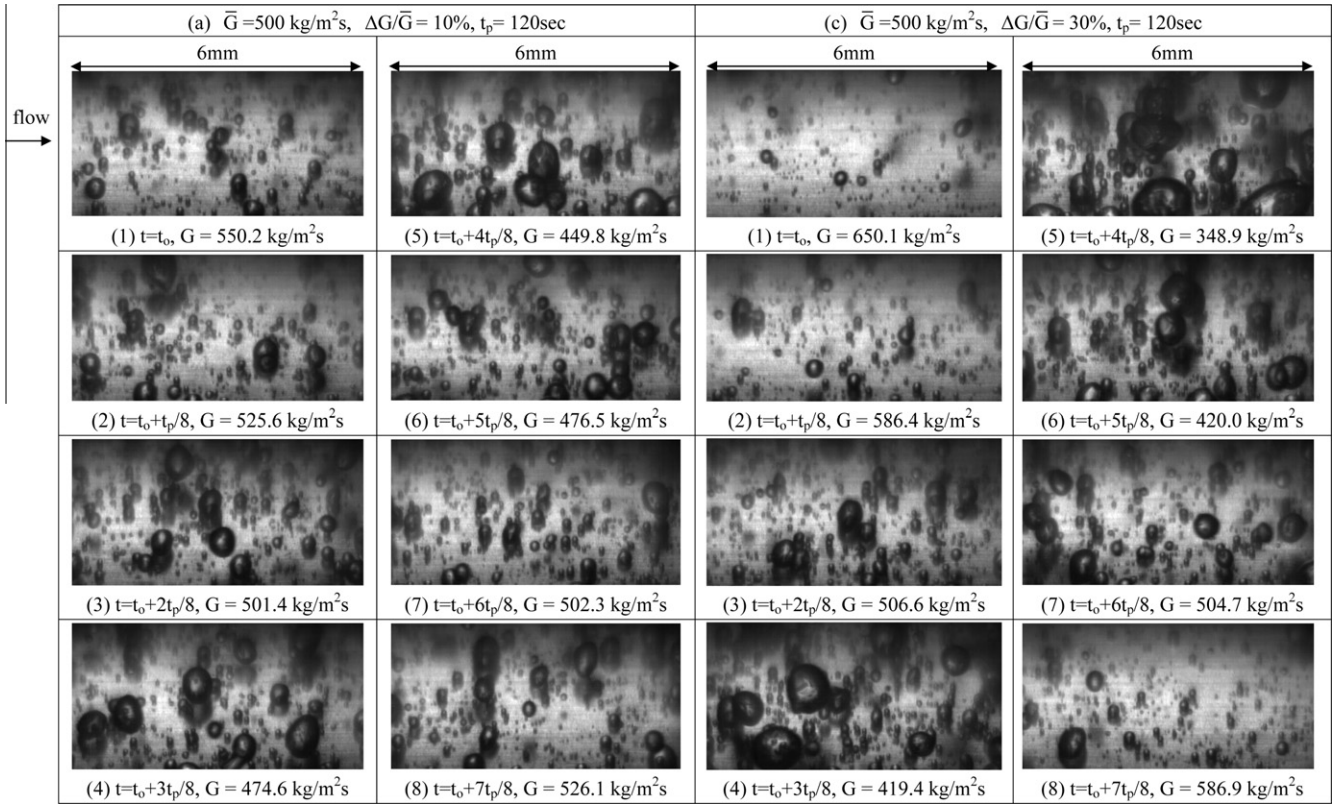

Fig. 7. Photos of bubbles in time periodic flow boiling of R-134a in a small region around the middle axial location at eight time instants in a typical periodic cycle at $\overline{T}_{sat}$ = 15 °C, q = 15 kW/m², and $\overline{G}$ = 500 kg/m² s for various $\Delta G/\overline{G}$ at t_p = 120 s.

the mass flux oscillation. Then, the bubble behavior in the intermittent flow boiling is demonstrated in Fig. 8. The results clearly indicate that initially at small t the instantaneous mass flux decreases with time but is still well above $\overline{G}$ no bubbles nucleate from the heated surface. The flow is in single-phase state. Note that the bubbles start to nucleate from the heated surface at a certain later time instant slightly before $t_0 + 3t_p/8$ at which the instantaneous mass flux is somewhat below $\overline{G}$, Besides, the number and size of the bubbles increase noticeably with time in the second quarter of the periodic cycle for the continuing decrease of the mass flux. Then in the third quarter of the periodic cycle the number and size of the bubbles diminish noticeably with time due to the increase of the mass flux. The bubbles cease to nucleate from the heated surface at a certain time instant slightly before $t_0 + 6t_p/8$ when the mass flux slightly exceeds $\overline{G}$ and bubble nucleation stops completely. Single-phase flow again diminates. We have to wait until the end of the first quarter of the next cycle to see the bubble nucleation appearing on the heated surface. The above processes repeat in each cycle. The precise instants of time at which the onset and termination of nucleate boiling take place vary with the flow conditions.

To be more quantitative on the bubble characteristics in the time periodic flow boiling due to the mass flux oscillation, we estimate the bubble departure diameter and frequency and the number density of the active nucleation sites on the heating surface in a typical periodic cycle at the middle axial location for the persistent flow boiling from the images of the boiling flow stored in the video tapes. Selected results from this estimation are manifested in Figs. 9–11 by presenting the effects of the amplitude and period of the refrigerant mass flux oscillation on the time dependent bubble characteristics for $\overline{G} = 500$ kg/m² s. In these plots the small time lag in the T_w oscillation is ignored. The data in Fig. 9 indicate that as the refrigerant mass flux oscillates time periodically, the bubble departure diameter also varies time periodically and to some degree like a triangular wave as the mass flux oscillation. More specifically, the size of the departing bubbles increases significantly in the first half of the periodic cycle in which G decreases with time. While in the second half of the cycle an opposite process is noted when G increases with time. Besides, the results in Fig. 9(a) show that at a larger amplitude of the mass flux oscillation the time variation of the bubble departure diameter is somewhat stronger. Meanwhile, the bubble departure diameter oscillates slightly stronger at a higher imposed heat flux. Moreover, the results in Fig. 9(b) indicate that to a certain degree the bubble departure diameter varies stronger with time for a longer period of the mass flux oscillation. Specifically, the amplitude of the d_p oscillation increases about 30% for t_p raised from 20 s to 120 s. This large change in the d_p oscillation amplitude with t_p causes the significant variation of the T_w oscillation amplitude with t_p, as already seen in Fig. 5(d). Furthermore, increases in the mean refrigerant mass flux and saturation temperature cause the departing bubbles to oscillate slightly stronger but do not change the wave form of the d_p variation with time (Fig. 9(c) and (d)). It is worth mentioning that even the size of the largest departing bubble is below 0.3 mm which is much smaller than the diameter of the outer glass pipe in the test section (D_p = 20.0 mm). Thus the observation of the bubble size through the curved surface of the glass pipe is not expected to produce significant error.

How the temporal variation of the bubble departure frequency is affected by the mass flux oscillation is shown in Fig. 10. Note that the bubble departure frequency also varies like a triangular wave. Besides, for an oscillating mass flux the bubbles depart from the heated surface at a decreasing rate in the first half of the periodic cycle in which the refrigerant mass flux reduces with time

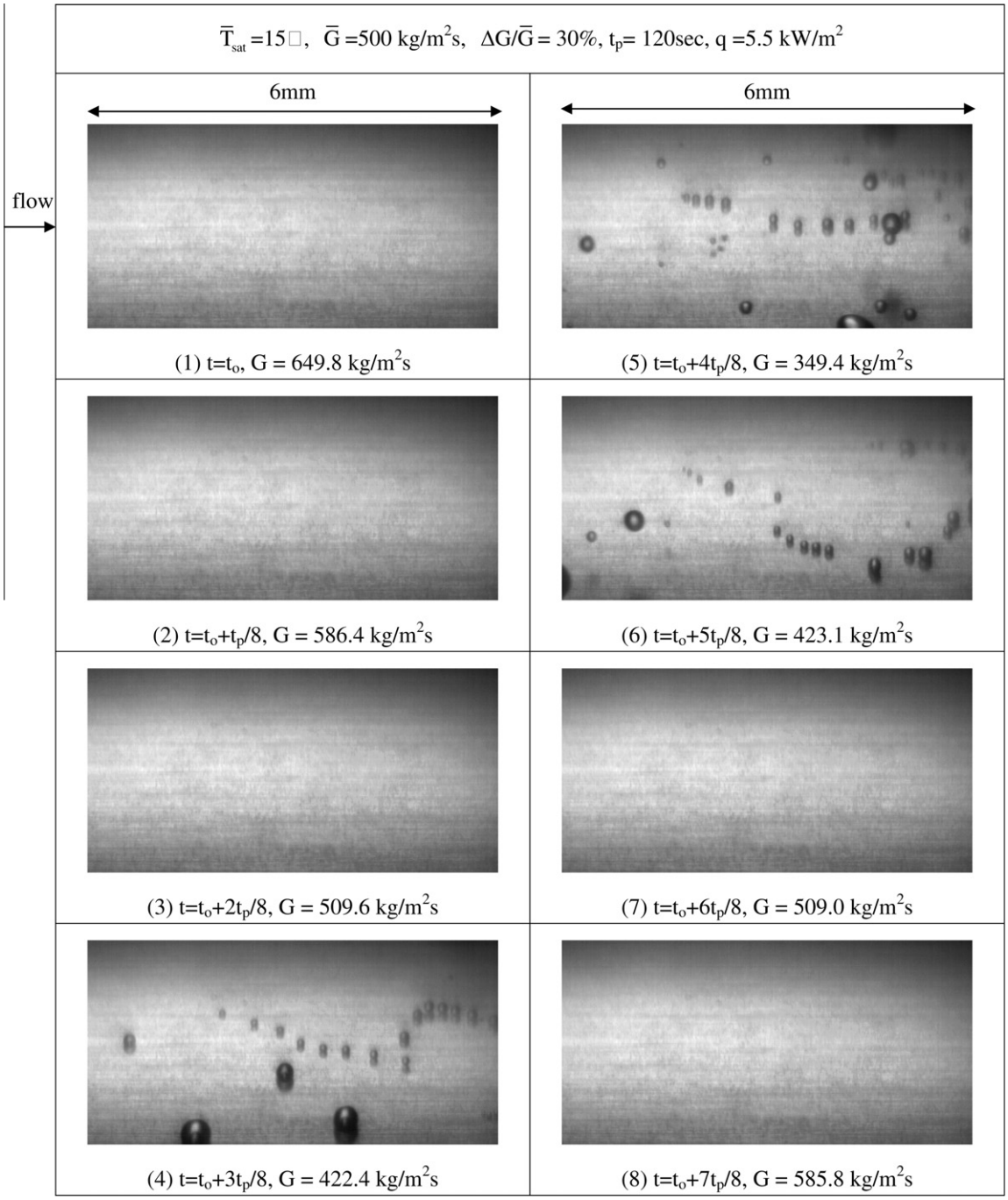

Fig. 8. Photos of bubbles in the time periodic intermittent flow boiling of R-134a in a small region around the middle axial location at eight time instants in a typical time periodic cycle for $\overline{T}_{sat}$ = 15 °C, $\overline{G}$ = 500 kg/m² s, q = 5.5 kW/m², $\Delta G/\overline{G}$ = 30%, and t_p = 120 s.

(Fig. 10(a)). Apparently, in the second half of the cycle in which the refrigerant mass flux increases the bubble departing rate rises. Moreover, the results in Fig. 10(a) indicate that at the larger amplitude of the mass flux oscillation the bubble departure frequency exhibits a stronger variation with time and at a higher q the oscillation in f is slightly stronger. Then, the results in Fig. 10(b) indicate that the bubble departure frequency is negligibly affected by the period of the mass flux oscillation. Finally, at higher $\overline{G}$ and $\overline{T}_{sat}$ the bubble departure frequency is in a stronger oscillation (Fig. 10(c) and (d)).

The time variations of the associated number density of the active nucleation sites affected by the mass flux oscillation presented in Fig. 11 clearly show that in the time periodic flow boiling the active nucleation site density also varies like a triangular wave. Besides, n_{ac} increases substantially with time in the first half of the periodic cycle in which the refrigerant mass flux decreases. The reverse process appears in the second half of the cycle in which the refrigerant mass flux rises. At the higher amplitude of the mass flux oscillation the temporal variation of n_{ac} is also stronger (Fig. 11(a)) and a higher imposed heat flux results in a slightly stronger oscillation in n_{ac}. But the effect of the period of the mass flux oscillation on the time variation of n_{ac} is small (Fig. 11(b)). Finally, n_{ac} oscillates slightly stronger at a lower $\overline{G}$ and a higher $\overline{T}_{sat}$ (Fig. 11(c) and (d)).

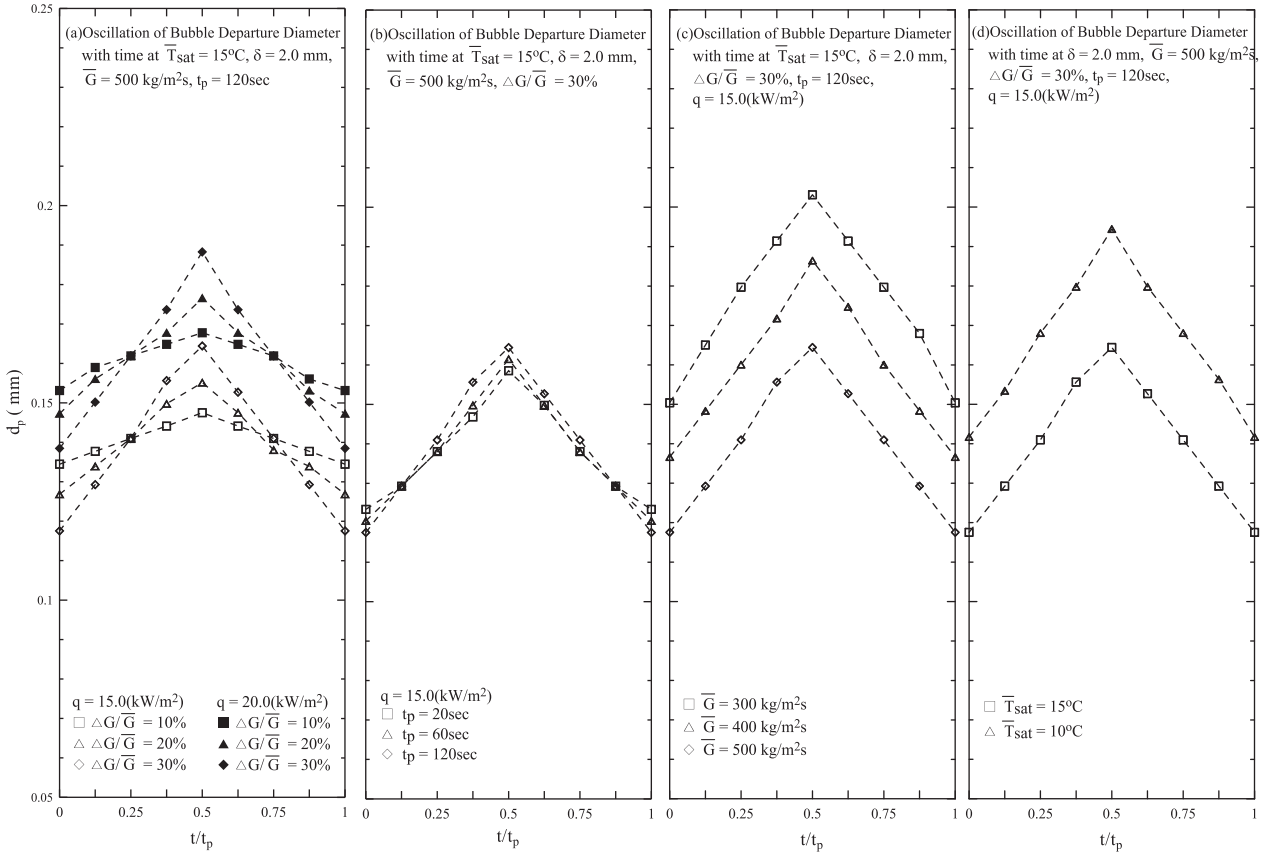

Fig. 9. Mean bubble departure diameter variations with time in a typical periodic cycle for various $\Delta G/\overline{G}$ at q = 15.0 and 20.0 kW/m² (a), t_p (b), $\overline{G}$ (c), and $\overline{T}_{sat}$ (d) at $\overline{G} = 500$ kg/m² s.

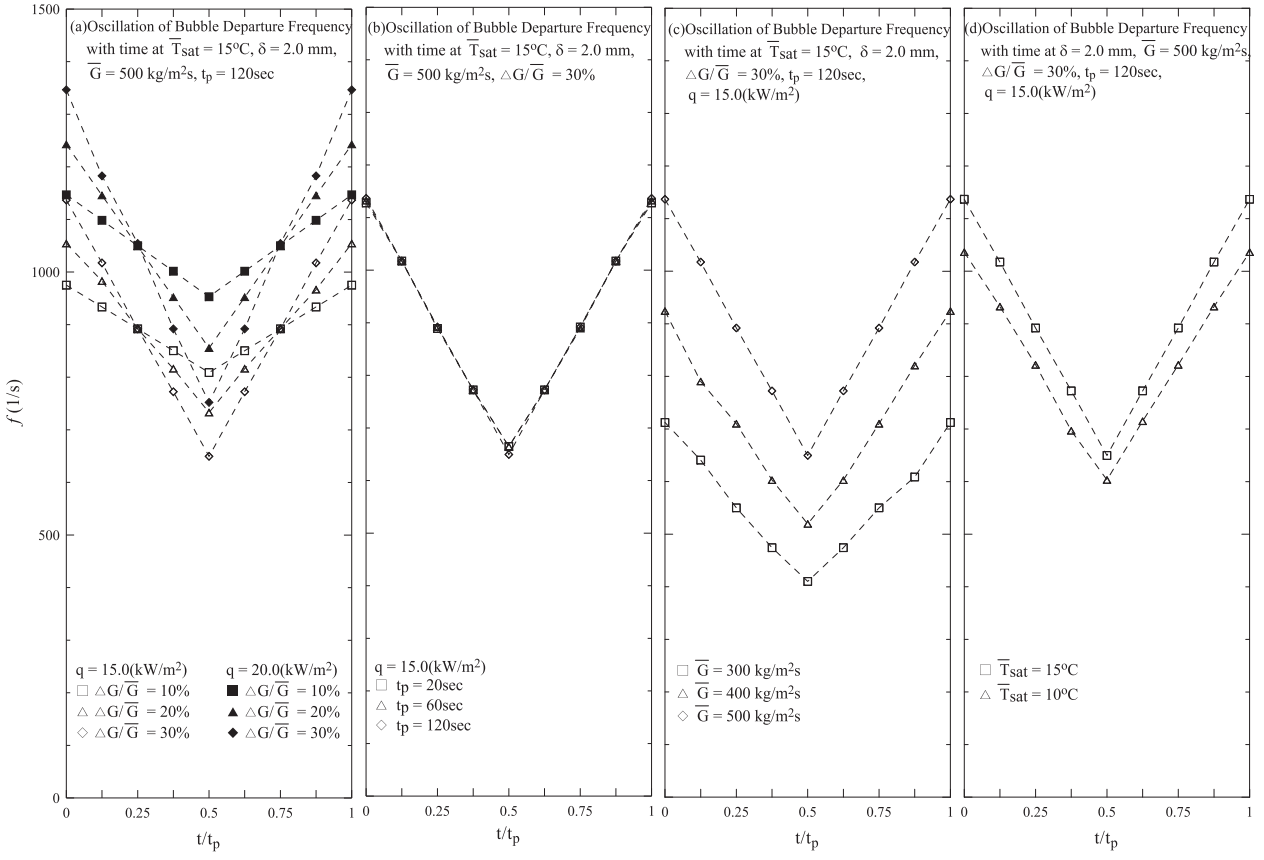

Fig. 10. Mean bubble departure frequency variations with time in a typical periodic cycle for various $\Delta G/\overline{G}$ at q = 15.0 and 20.0 kW/m² (a), t_p (b), $\overline{G}$ (c), and $\overline{T}_{sat}$ (d) at $\overline{G} = 500$ kg/m² s.

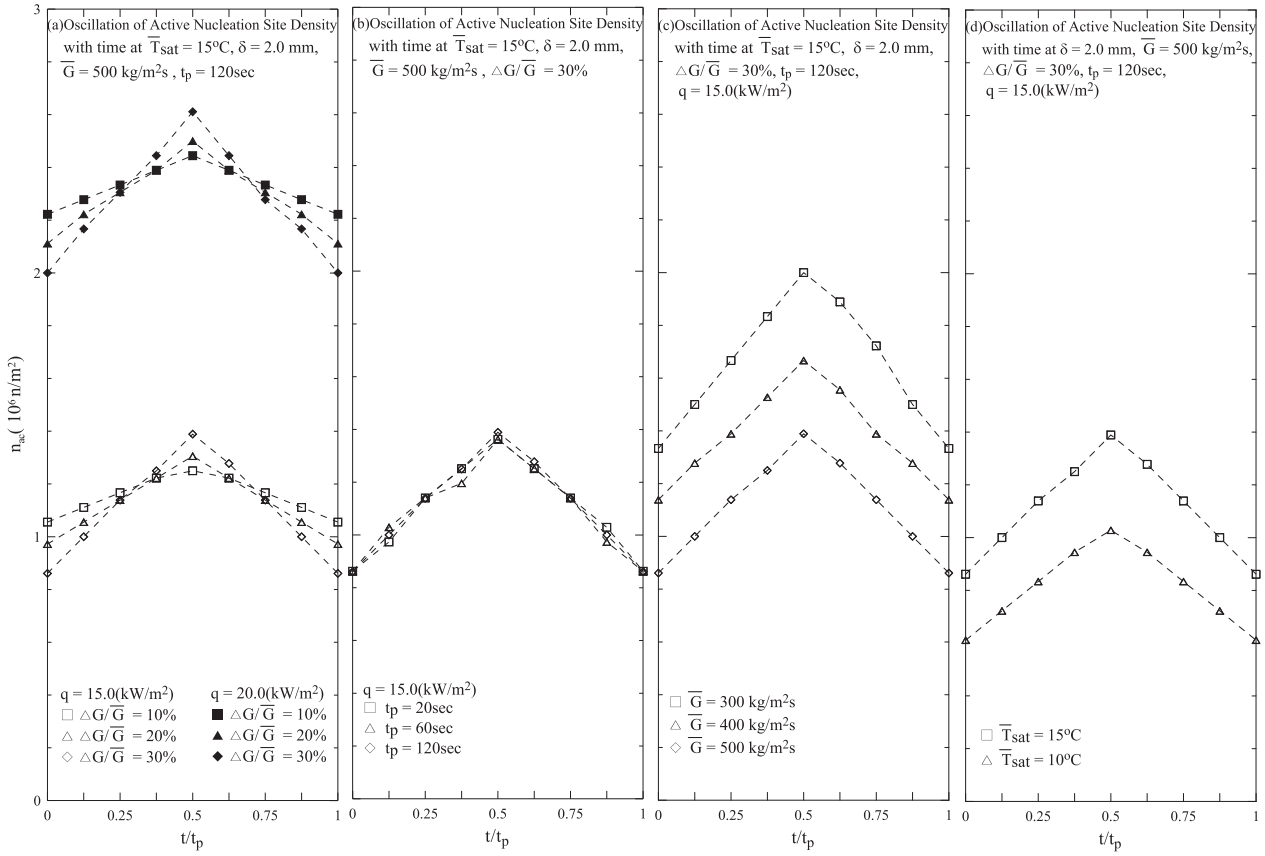

Fig. 11. Mean active nucleation site density variations with time in a typical periodic cycle for various $\Delta G/\overline{G}$ at q = 15.0 and 20.0 kW/m² (a), t_p (b), $\overline{G}$ (c), and $\overline{T}_{sat}$ (d) at $\overline{G}$ = 500 kg/m² s.

Based on the data in Figs. 9–11, the dependence of the quantitative bubble characteristics on the R-134a mass flux oscillation can be approximately expressed as $d_p \propto G^{-a}$, $f \propto G^{b}$ and $n_{ac} \propto G^{-c}$ when the short time lag in the T_w oscillation is neglected. Here the exponents *a*, *b,* and *c* range respectively from 0.37 to 0.42 , 0.93 to 0.99, and 0.46 to 0.65. Note that the latent heat transfer resulting from bubble nucleation in the persistent boiling q_b is proportional to d_p^3, f and n_{ac}, as discussed in the previous study [26]. Thus, $q_b \propto G^{-d}$, here d varies from 0.58 to 0.98. This result clearly indicates that the flow boiling heat transfer gets better at decreasing refrigerant mass flux since q_b prevails in the boiling heat transfer. This in turn causes the heated wall temperature to decrease at decreasing refrigerant mass flux and vice versa in the time periodic flow boiling, as already seen from Fig. 3. Besides, the dominant effect of the mass flux oscillation on the boiling heat transfer comes from the very strong influence of the mass flux on the bubble departure size.

5. Concluding remarks

The heat transfer data for the time periodic flow boiling of R-134a resulting from the refrigerant mass flux oscillation in the narrow annular duct have been presented here along with the bubble behavior. Effects of the mean level and oscillation amplitude and period of the refrigerant mass flux on the time periodic R-134a flow boiling have been investigated. The major results obtained here can be summarized in the following.

(1) The time-average boiling curves and heat transfer coefficients for the time periodic flow boiling of R-134a are not affected to a noticeable degree by the amplitude and period of the refrigerant mass flux oscillation.

(2) The heated pipe wall temperature, bubble departure diameter and frequency and active nucleation site density also oscillate periodically in time and at the same frequency as the mass flux oscillation. Experiments also show that the resulting oscillation amplitudes of the wall temperature get larger for a longer period and a larger amplitude of the mass flux oscillation. Besides for a larger amplitude of the mass flux oscillation, stronger oscillations in the bubble characteristics, such as d_p, f and n_{ac}, are noted. But f and n_{ac} are only slightly affected by the period of the mass flux oscillation. A short time lag in the wall temperature oscillation is also noted. Moreover, the bubbles become smaller and more dispersed in the flow when the refrigerant mass flux increases with time. The opposite processes take place for a decreasing refrigerant mass flux. Furthermore, reductions in the size of the departing bubbles and active nucleation site density and augmentation in the bubble departure frequency result in the time duration in which the mass flux is rising. When the mass flux is sinking the opposite processes occur.

(3) Increases in the bubble departure size and active nucleation site density at decreasing refrigerant mass flux overwhelms the decrease in the bubble departure frequency. This in turn causes an increase in the latent heat transfer and a drop in the heated wall temperature at decreasing *G*, opposite to that in the single-phase flow.

(4) When the imposed heat flux over the heated surface is close to the heat flux corresponding to that for the onset of stable flow boiling, intermittent flow boiling appears. A flow regime map and an empirical correlation are given to delineate the boundaries separating different flow regimes in the annular duct.

Acknowledgment

The financial support of this study by the engineering division of National Science Council of Taiwan, R.O.C. through the contract NSC 96-2221-E-009-133-MY3 is greatly appreciated.

References

[1] Z.Y. Bao, D.F. Fletcher, B.S. Haynes, Flow boiling heat transfer of Freon R11 and HCFC123 in narrow passages, Int. J. Heat Mass Transfer 43 (2000) 3347–3358.
[2] T.N. Tran, M.W. Wambsganss, D.M. France, Small circular- and rectangular-channel boiling with two refrigerants, Int. J. Multiphase Flow 22 (1996) 485–498.
[3] B. Agostini, A. Bontemps, Vertical flow boiling of refrigerant R134a in small channels, Int. J. Heat Fluid Flow 26 (2005) 296–306.
[4] S.G. Kandlikar, M.E. Steinke, Flow boiling heat transfer coefficient in minichannels – correlation and trends, in: Proceedings of the Twelfth International Heat Transfer Conference 3 (2002) 785–790.
[5] S. Lin, P.A. Kew, K. Cornwell, Two-phase heat transfer to a refrigerant in a 1 mm diameter tube, Int. J. Refrig. 24 (2001) 51–56.
[6] B. Watel, Review of saturated flow boiling in small passages of compact heat exchangers, Int. J. Therm. Sci. 42 (2003) 107–140.
[7] T. Otsuji, A. Kurosawa, Critical heat flux of forced convection boiling in an oscillating acceleration field: I – general trends, Nucl. Eng. Design 71 (1982) 15–26.
[8] T. Otsuji, A. Kurosawa, Critical heat flux of forced convection boiling in an oscillating acceleration field: II – contribution of flow oscillation, Nucl. Eng. Design 76 (1983) 13–21.
[9] S. Kakac, T.N. Veziroglu, M.M. Padki, L.Q. Fu, X.J. Chen, Investigation of thermal instabilities in a forced convection upward boiling system, Exp. Therm. Fluid Sci. 3 (1990) 191–201.
[10] M.M. Padki, H.T. Liu, Kakac, Two-phase flow pressure-drop type and thermal oscillations, Int. J. Heat Fluid Flow 12 (1991) 240–248.
[11] Y. Ding, S. Kakac, X.J. Chen, Dynamic instabilities of boiling two-phase flow in a single horizontal channel, Exp. Therm. Fluid Sci. 11 (1995) 327–342.
[12] O. Comakli, S. Karsli, M. Yilmaz, Experimental investigation of two phase flow instabilities in a horizontal in-tube boiling system, Energy Convers. Manage. 43 (2002) 249–268.
[13] P.R. Mawasha, R.J. Gross, Periodic oscillations in a horizontal single boiling channel with thermal wall capacity, Int. J. Heat Fluid Flow 22 (2001) 643–649.
[14] Q. Wang, X.J. Chen, S. Kakac, Y. Ding, Boiling onset oscillation : a new type of dynamic instability in a forced-convection upflow boiling system, Int. J. Heat Fluid Flow 17 (1996) 418–423.
[15] D. Brutin, F. Topin, L. Tadrist, Experimental study of unsteady convective boiling in heated minichannels, Int. J. Heat Mass Transfer 46 (2003) 2957–2965.
[16] D. Brutin, L. Tadrist, Pressure drop and heat transfer analysis of flow boiling in a minichannel: influence of the inlet condition on two-phase flow stability, Int. J. Heat Mass Transfer 47 (2004) 2365–2377.
[17] J. Shuai, R. Kulenovic, M. Groll, Pressure drop oscillations and flow patterns for flow boiling of water in narrow channel, in: Proceedings of International Conference on Energy and the Environment, Shanghai, China, May 22–24, 2003.
[18] S. Kakac, B. Bon, A review of two-phase flow dynamic instabilities in tube boiling systems, Int. J. Heat Mass Transfer 51 (2008) 399–433.
[19] L. Tadrist, Review on two-phase flow instabilities in narrow spaces, Int. J. Heat Fluid Flow 28 (2007) 54–62.
[20] C.P. Yin, Y.Y. Yan, T.F. Lin, B.C. Yang, Subcooled flow boiling heat transfer of R-134a and bubble characteristics in a horizontal annular duct, Int. J. Heat Mass Transfer 43 (2000) 1885–1896.
[21] R. Situ, Y. Mi, M. Ishii, M. Mori, Photographic study of bubble behaviors in forced convection subcooled boiling, Int. J. Heat Mass Transfer 47 (2004) 3659–3667.
[22] R. Maurus, V. Ilchenko, T. Sattelmayer, Automated high-speed video analysis of the bubble dynamics in subcooled flow boiling, Int. J. Heat Fluid Flow 25 (2004) 149–158.
[23] S.H. Chang, I.C. Bang, W.P. Baek, A photographic study on the near-wall bubble behavior in subcooled flow boiling, Int. J. Therm. Sci. 41 (2002) 609–618.
[24] V.H. Del, M. Balle, D.B.R. Kenning, Subcooled flow boiling at high heat flux, Int. J. Heat Mass Transfer 28 (1985) 1907–1920.
[25] T. Okawa, T. Ishida, I. Kataoka, M. Mori, An experimental study on bubble rise path after the departure from a nucleation site in vertical upflow boiling, Exp. Therm. Fluid Sci. 29 (2005) 287–294.
[26] Y.M. Lie, T.F. Lin, Saturated flow boiling heat transfer and associated bubble characteristics of R-134a in a narrow annular duct, Int. J. Heat Mass Transfer 48 (2005) 5602–5615.
[27] S.W. Churchill, H.H.S. Chu, Correlating equations for laminar and turbulent free convection from a horizontal cylinder, Int. J. Heat Mass Transfer 18 (1975) 1049–1053.
[28] S.J. Kline, F.A. McClintock, Describing uncertainties in single-sample experiments, ASME Mech. Eng. 75 (1953) 3–12.
[29] V. Gnielinski, New equations for heat and mass transfer in turbulent pipe and channel flow, Int. Chem. Eng. 16 (1976) 359–368.